Scanning Microscopy

Volume 1994
Number 8 *The Science of Biological Microanalysis*

Article 24

12-20-1994

The Principles of Proton Probe Microanalysis in Biology

G. J. F. Legge
The University of Melbourne, Australia

M. Cholewa
The University of Melbourne, Australia

Scanning Microscopy Supplement 8, 1994 (pages 295-315) 0892-953X/94$5.00+.25
Scanning Microscopy International, Chicago (AMF O'Hare), IL 60666 USA

THE PRINCIPLES OF PROTON PROBE MICROANALYSIS IN BIOLOGY

G.J.F. Legge* and M. Cholewa

Micro Analytical Research Centre, School of Physics.
The University of Melbourne, Australia 3052

(Received for publication March 29, 1994, and in revised form December 20, 1994)

Abstract

The proton microprobe, more correctly described as an ion microprobe which operates at MeV energies, complements its parent instrument the electron microprobe. This paper compares the basic principles and performance of the two instruments and relates the evolution of biological analysis on such ion microprobes to that on electron microprobes, covering the development of sample handling techniques and of data handling techniques and comparing beam damage studies. The paper describes the variety of techniques available to the ion microprobe - the initial techniques of Energy Dispersive X-ray analysis, Rutherford Back Scattering and Nuclear Reaction Analysis and the rapid evolution of new techniques, from Scanning Transmission Ion Microscopy to 3-dimensional tomography. All of these new techniques required the advanced computerised data handling which has been a feature of ion microprobe development.

Key Words: Proton microprobe, Rutherford Back Scattering, Nuclear Reaction Analysis, Scanning Transmission Ion Microscopy.

*Address for correspondence:
G.J.F. Legge
Micro Analytical Research Centre, School of Physics,
The University of Melbourne, Australia 3052
Phone Number: +61-3-3445433
Fax Number: +61-3-3474783

Introduction

This paper discusses the early development of both the proton microprobe (PMP) and its application to biology. The close analogy with the electron microprobe (EMP) is emphasised and the significant differences analysed. The major impact of early computerisation on the PMP is shown and its effect in encouraging the later development of many new techniques is discussed. Data are selected to illustrate the techniques and the paper does not attempt to give a wide coverage of biological applications of the PMP; for such a coverage, it should be read in conjunction with several other papers on this subject delivered at this conference.

The first focused PMP was developed because the field of elemental microanalysis had a problem. Its major analytical instrument, the electron microprobe (EMP), was limited in sensitivity by the continuous background of bremsstrahlung inherent in all X-ray spectra. Pierce's group at the British AEC, Harwell (Pierce *et al.*, 1966, 1968) and Bird's group at the Australian AEC, Lucas Heights (Mak *et al.*, 1966; Price and Bird, 1969) performed microanalysis with beams of high energy ions collimated down to diameters of a few hundred micron. Then, in 1970, Cookson, Ferguson and Pilling, at Harwell (Cookson and Pilling, 1970; Cookson *et al.*, 1972) took the major step of focusing such beams down to a diameter of 4 micron. This first PMP had front and back viewing microscopes (for setting up specimens) and was equipped initially for Rutherford Back Scattering (RBS) analysis, Nuclear Reaction Analysis (NRA) and (in 1971) Particle Induced X-ray Emission (PIXE) analysis. It has been used ever since principally as a powerful tool for materials analysis. As such, it has operated most frequently with beam particles heavier than the proton, and in 1973 the name was changed to ion microprobe (IMP).

An investigation into the analysis of biological material with a PMP commenced at Harwell in 1973, when one of the authors (G.J.F.L) commenced a year of work devoted to this purpose (Legge, 1974; Cookson and Legge, 1975). The success of these preliminary investigations led to the immediate establishment of a PMP at Melbourne specifically designed for biological

applications. It came into operation early in 1976 (Legge *et al.*, 1979), as did the PMP at Heidelberg (Nobiling *et al.*, 1977) also to be used extensively for biological work. Meanwhile, a PMP had been assembled in 1973 at Studsvik (Brune *et al.*, 1977) later to be used by Lindh for biological work (Lindh *et al.*, 1978). In 1974, Cho *et al.*, reported the assembly of an IMP for biomedical applications (Cho *et al.*, 1974), but this work was not continued. A collimated PMP set up at MIT with the beam extracted (Horowitz *et al.*, 1976) and used to examine biological tissues should also be mentioned in this early history. PMP's set up in 1977 at the Nuclear Research Centre in Karlsruhe (Heck, 1979), at the Ruhr University in Bochum (Wilde *et al.*, 1978) and at the Institute of Nuclear Sciences in Lower Hutt NZ (Coote *et al.*, 1978) have also been used for several biological studies. Thus, over the period of 1973 to 1977, there was a strong movement into this new field of biological PMP studies and this has continued.

The microprobe at Lower Hutt had been named a Nuclear Microprobe (NMP) and since then this name has become popular within Nuclear Research Institutes. Many PMP and IMP papers from Harwell had been based mainly on NRA techniques and in 1983 there was a second change of name (this time to NMP). Although our group, like most university groups, always used the original name of PMP, it would be more logical to use the name IMP - the only name which is truly descriptive of this very versatile instrument, which covers all its uses and modes of operation and which is again becoming popular as a result of the many new nonnuclear techniques which call for microbeams of ions other than protons. However, we shall continue to use the name PMP in this paper, in order to avoid confusion with the low velocity (or sputter) ion microprobe. It will become apparent later why velocity, not energy, is the significant parameter in discussing microprobes.

We shall introduce the discussion of biological microanalysis on a PMP by some general remarks based on fundamental physical principles; this will enable us to draw several conclusions with regard to its strengths and weaknesses as compared to similar analysis with an EMP.

Comparison with the Electron Microprobe

Efficiency of elemental analysis

Elemental analysis with the PMP is mostly performed by Energy Dispersive X-ray Analysis (EDX), often referred to as Particle Induced X-ray Emission (PIXE), and in this mode the PMP is directly comparable with the electron microprobe (EMP). The cross section for ionization of, and hence characteristic X-ray emission from, an atom is a maximum when a charged particle passes with a velocity comparable to the orbital velocity of the electron to be detached. Since the electron and proton carry the same (though opposite) charge, they will exert a Coulomb force of the same magnitude on an electron in their vicinity. Hence we may expect that the EMP and PMP will be equally efficient in performing EDX if operated with the same velocity particles. This means that the EMP should operate at an energy somewhat higher than the highest ionization energy of interest - higher because this would be a threshold energy. At the same velocity, the proton would have 1840 times the energy. However, as this is far above any threshold energies, the PMP is usually operated somewhat below the energy for maximum cross section. Nevertheless, the energies are such that a charged particle accelerator of several MV is required - 3 MV being close to optimum for the detection of most elements as shown by Folkmann *et al.* (1974a,b).

Lateral resolution

In order to focus such a high momentum particle beam, strong focussing quadrupole lenses are required, in place of the weak focussing cylindrical lenses employed in the EMP. Even so, the lens, and consequently the focal length, is long. Therefore the ion optical path is long (to achieve reasonable demagnification). The longer focal length leads directly to larger values for the lens aberration coefficients and the present unavailability of high brightness ion sources compounds the problem, since it requires the use of large source and lens apertures. Consequently the lateral resolution for EDX with the PMP is limited to not much less than a micron, it being generally agreed that EDX in a PMP requires a beam current of at least 100 pA. However, this lateral resolution is not a fundamental limitation, stemming mostly from the low brightness of currently available ion sources. The ions of the PMP beam suffer much less scattering by the atoms of a specimen than the electrons of the EMP beam. Consequently a micron sized proton beam entering a hydrocarbon matrix will retain that resolution over a depth of more than 10 microns, in contrast to an electron beam, which loses resolution rapidly in a thick specimen.

Depth resolution

EDX is not a sensitive tool for depth profiling. Nevertheless the effective depth of its analytical analysis is confined to that for which the charged particles of the beam have sufficient velocity to readily ionize atoms of the specimen. It is obvious from the discussion of the section on "Efficiency of elemental analysis" that the critical parameter is velocity - not energy. However, the

low energy electrons of an EMP have much less effective penetration depth than ions of the same velocity in a PMP. Consequently, in a PMP the effective depth of analysis, at least for light elements, is limited mostly by the absorption of their low energy X-rays in the matrix, and not by the range of the proton beam. This large depth of analysis will enhance the yield of X-rays, but can also result in the excitation of structure underlying that of interest, unless this is avoided by appropriate selection of section thickness in preparing the specimen. See, however, the later comments on 3-D structure.

Limits of elemental detection

It is obvious that the use of high energy ions as an elemental probe leads to some complexities in the handling of the beam. However this is more than offset by the accompanying benefits. As indicated above, the cross section for excitation of an element's characteristic X-radiation in EDX is similar when performed with electrons or protons of similar velocities. However, the detection limit for EDX depends on the ratio of this cross section to that for exciting bremsstrahlung, the continuous background of radiation underlying the spectrum of characteristic radiation. Classically, just as a proton and electron of similar velocities have similar ionization cross sections for any atom which they approach, so do they themselves receive similar Coulomb impulses from the atomic nuclei. The acceleration of the proton will then be less by a factor of 1840 and the bremsstrahlung radiation from the proton will have an amplitude less by the same factor. The intensity will be less by the square of the same factor. Thus direct bremsstrahlung (projectile-nucleus) from protons or heavier ions will be negligible. The bremsstrahlung that is seen is mostly secondary radiation, coming from the knock-on electrons (delta rays) as they are accelerated (electron-projectile) and decelerated (secondary electron) in the specimen, and it does not extend significantly to high energies. This is illustrated in Figure 1, a theoretical calculation compared with direct measurement of the background radiation spectrum in a microprobe, coming from a beam of 3 MeV protons passing through a thin carbon foil (Guy, 1977). Note that the intensity scale is logarithmic, emphasising the rapid fall in intensity with X-ray energy. In contrast, a typical bremsstrahlung spectrum from an electron beam (shown dotted) has comparable yield for low energy radiation but without the dramatic decline in strength at high energies. Thus EDX in a PMP is an ideal technique for elemental microanalysis of biological material, because the important trace elements are mostly the so-called heavy metals with K X-ray energies above most of the bremsstrahlung from the light matrix.

Because the limits of detection are set by the bremsstrahlung background, the PMP in general has detection limits about 2 orders of magnitude better than those of the EMP. It must be emphasised that this comes from a lower background and not from a higher elemental signal. Therefore the PMP will often require long collection times to make these very sensitive measurements (until such time as the beam brightness is greatly improved) - see the later section on data handling. The detection limit of the PMP is often set by the statistics accumulatable within a reasonable time.

Damage

Since both X-ray production and beam particle energy loss processes are similar for protons and electrons of comparable velocities, we should also expect the PMP and EMP to yield similar information for the same degree of damage to the specimen, at least in the high velocity region where so-called electron stopping predominates. The situation is not comparable near the end of an ion's range, where nuclear stopping predominates; however the above approximation should hold for thin specimens. There is further discussion of damage later under elemental losses.

Light elements and normalisation

Unlike the backscatter signal in an EMP, each backscattered beam particle in a PMP carries information on the specimen, in its energy. When an ion strikes an atom and scatters at some known angle (set by the detector position), it will exchange kinetic energy and it will also lose energy in traversing the specimen on entry and exit. Hence, the energy of the scattered ion will be determined by the beam energy, the ratio of the ions mass to that of the scattering atom and the depth of the scattering atom beneath the surface of the specimen. For many specimens, Rutherford Back Scattering (RBS) is the most powerful quantitative tool for depth profiling, particularly that of heavy elements in a light matrix; and, for this purpose, RBS had been established from the beginning on the PMP at Harwell. However, the cross section for RBS is much lower than that for PIXE and depth profiling is not usually required in thin biological specimens. In the early biological trials at Harwell, therefore, the Si(Li) detector was mainly used. However, in a PMP, it is necessary to protect the Si(Li) crystal from the very energetic and damaging backscattered ions and the foil required to stop these ions also absorbs the X-rays from light elements. Therefore RBS was investigated as a means of detecting the light elements C,N and O, which are so abundant in biological specimens; and, by installing a detector at a forward angle of 45°, it was also shown that even H could be

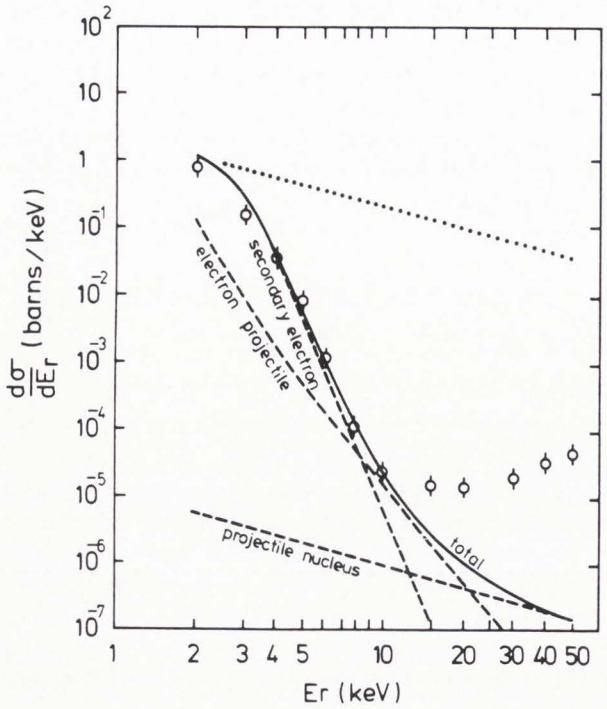

Figure 1: The theoretically predicted spectrum of X-rays from primary and secondary bremsstrahlung in C is compared with experimental measurements with a proton microbeam (Guy, 1977). The beam energy is 3 MeV and the measurements were made with a thin kapton foil as target. In comparison, the typical yield of bremsstrahlung from electron irradiation (shown dotted) exhibits a much more gradual decrease with energy.

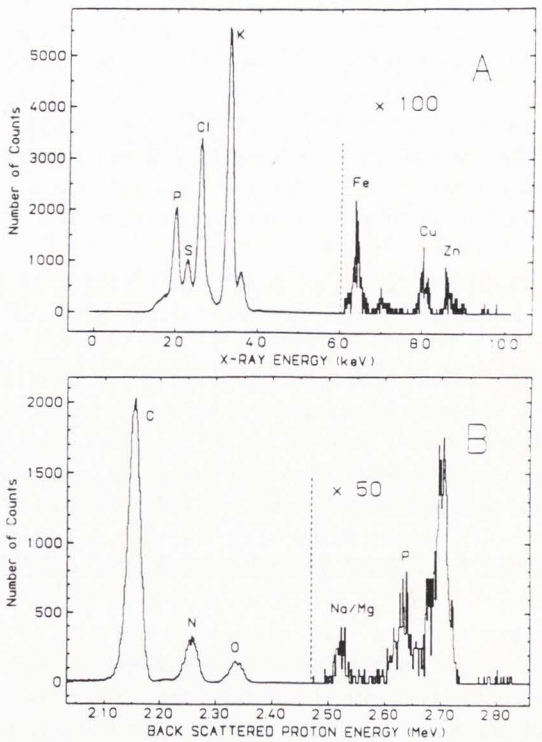

Figure 2: Spectra of X-rays (A) and of backscattered protons (B) from a single Menkes fibroblast. Total beam charge was 2.1 μC. Note the offset baseline in each spectrum, there being negligible background in each case.

readily detected in such thin biological specimens by Rutherford Forward Scattering (RFS) (Legge *et al.*, 1979). Information on the light elements may be needed to measure deterioration of the specimen matrix by means of elemental loss (see later under damage), measure protein in the sample by means of its N content (Cookson and Legge, 1975) or normalise the heavy elemental abundances to specimen mass - the bremsstrahlung background from the thin specimen provided a measurement of specimen thickness for normalisation of elemental yields, a technique already made standard on the EMP by Hall (Hall, 1968) but, with the low bremsstrahlung levels on the PMP, a more accurate normalisation could be obtained with the direct measurement of light elements by RBS. Figure 2 shows the total X-ray spectrum and total RBS spectrum from a single skin fibroblast cell that had been scanned with a beam of 3 MeV protons. The cell carried the Menkes mutation and hence had abnormally high Cu level. For a normal cell, the yield of Cu K_α radiation, though still measurable, was but a small fraction of the yield of Fe K_β radiation - visible to the right of the Fe (K_α) peak. Note the low background of bremsstrahlung at high energies and that the scale has been magnified by 100. A low background and good elemental peak separation is also seen in the RBS spectrum.

RBS was used also to measure Na in the above cell (Allan *et al.*, 1991), where the Na X-rays could not enter the Si(Li) detector and the cross sections were too low to enable detection of Na by Nuclear Reaction Analysis (NRA). However NRA can be used in some cases where the cross sections are unusually high, as in the detection of F by the reaction $^{19}F(p,\alpha\sigma)^{16}O$, (Coote and Sparks, 1981).

The preparation of specimen

Generally, as for the EMP, specimens are snap frozen, thick specimens are cryosectioned and all specimens are freeze dried in a very clean vacuum system. Maintaining elemental purity is of utmost importance and preservation of morphology and elemental distribution is essential only to the limit of the PMP's spatial resolution. The preparation of biological tissue for a trace element analysis on the PMP has been

discussed specifically by Kirby and Legge (Kirby and Legge, 1993) and discussions are also included in most papers on biological applications (Legge *et al.*, 1982; Malmqvist, 1986; Watt and Grime, 1988; Lindh, 1988, 1991).

A vast body of literature exists on the preparation of biological samples for the EM and there is a rapidly growing body of literature for the EMP. It is important that PMP users become familiar with this literature and also note the differences in EMP and PMP requirements. These may be summarised as follows:

(i) The ability of the PMP to detect trace elements requires greater precaution in the prevention of elemental losses or contamination at all stages of the specimen's preparation. Samples must be dried, as for the EMP, but the need to avoid all forms of chemicals - fixatives, drying agents, embedding materials, stains etc., is even greater for the PMP, because of the greater sensitivity to impurities.

(ii) The need to detect such elements, though with less beam current available in the PMP, requires maximum efficiency and thicker specimens. Fortunately, with the generally larger spot size but diminished beam scattering, such thicker specimens are appropriate to the PMP.

(iii) Sample area is frequently greater in the PMP.

(iv) With a cryomicrotome, the thicker the section to be cut and the larger the area of the block, the higher must be the cutting temperature.

(v) The larger dimensions of the sections to be cut for the PMP may require a larger block to be cryofixed. This increases the incidence and size of ice crystals. Fortunately, the poorer resolution of the PMP makes this less significant.

As with the EMP, plastic foil specimen supports are required - as thin as possible (to minimise the bremsstrahlung) and free from impurities. Commercial plastic foils were generally found to be too thick (several micron) or contaminated and foils prepared in the laboratory were fragile and often contained traces of solvent chemicals. This problem was solved when T.A. Hall of Cambridge University kindly supplied the formula and material for preparing the very clean and strong thin films of nylon, which he had developed for biological work with the EMP (Echlin and Moreton, 1974). It was found that specimens, including foils, generally developed yellow discoloration in areas exposed to the beam. Since these marks sometimes disappeared with time (weeks), it seemed that they were due to the production of colour centres by ionization, and not to contamination - a conclusion reinforced later by similar behavior in a cleaner high vacuum. The only disadvantage of nylon as a support seems to be its high N content, which would be a problem when that element was of significance.

Instrumentation

In comparison with an EMP, the PMP tends to be long, horizontal, frequently of higher vacuum, complex in its instrumentation because of the many techniques available and more highly computerised in its data handling.

As an example, the PMP at Melbourne has a metal-sealed ion-pumped ultra-high vacuum (UHV) system mounted on a single strong girder, of 9 m length, with insulation against mechanical vibration in the supporting pillars. The lens which, like the original Harwell lens, is a "Russian Quadruplet" of magnetic quadrupole lenses (Dymnikov *et al.*, 1963), forms a demagnified image of an object diaphragm at the specimen. The beam from a 5 MV charged particle accelerator is focussed onto this object diaphragm. The UHV specimen chamber, shown in Figure 3, contains 6 concentric rings which can be rotated around the specimen - these support RBS and RFS detectors, mirrors and other devices which need to be positioned within the chamber without breaking the vacuum. A Si(Li) detector is provided for EDX work and the specimen is supported from an X-Y-Z-θ-Φ goniometer. The turret of rear-viewing microscope objective lenses (inside the chamber) is also operated via an UHV mechanism. The movements required within the tight geometry of the chamber dictated the provision of a large viewport (one side of the specimen chamber) - of inestimable benefit to all work. This chamber is ion-pumped. Specimens can be changed through a 5 cm gate valve to the turbomolecular-pumped vacuum lock visible below the chamber.

Scanning

The discussions of scanning and data handling are not included in the above comparison of instruments, because the principles covered are general ones, of relevance to all instruments.

The original scanning system on the Harwell PMP had 2 free running analogue triangular wave generators. The PMP at Melbourne adopted a similar scanning technique, because it moved the beam rapidly over the specimen to give a quick image for a weak biological signal and there was no "flyback" period to require gating of signals. Of even greater significance was that, although ionization damage to the specimen could not be affected, thermal damage hopefully could be minimised by the rapid movement of the beam spot; but it also required high frequency scanning and this in turn required that the scan signal not be generated directly by

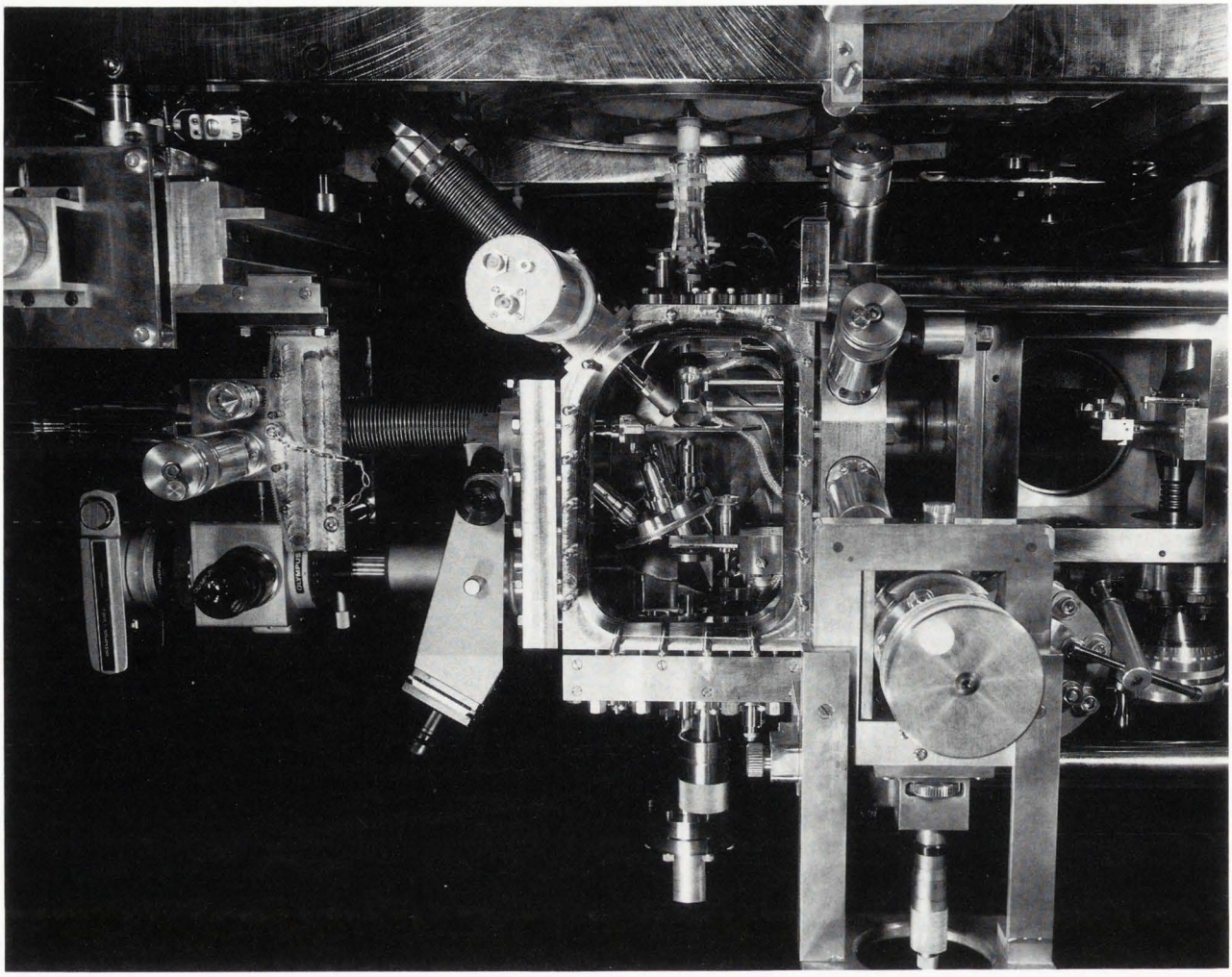

Figure 3: UHV chamber of a proton microprobe with a vacuum lock below. The ion beam enters from the lens just visible on the right of the photograph.

a computer (since the computer would have to generate scan signals at a rate equal to twice the scanning resolution times the scanning frequency). High frequency scanning required rapid triggering on detected radiation signals and careful timing. This was aggravated by the use of triangular waves in both scanning directions, because it meant that the scan moved through each point in 4 directions; as a result, timing errors would lead to quadruple imaging of every point, with the 4 "spots" moving further apart as the scanning frequency or the timing error increased. Very fast scanning could not be done with movement of the specimen stage or with signals added to the lens currents. The original oscillators operated up to 1 kHz and a system operating up to 20 kHz was installed in 1980.

Data Handling

The development of biological work with the PMP required a major revision in the handling of data (Legge, 1977). Till this time, there had been a standard method of collecting data from any scanning instrument. If a spectrum was required, fixed spot (unscanned) mode was used otherwise the spectrum collected would apply to the whole of the scanned area. If maps associated with various peaks in the spectrum (and therefore with elemental distributions in our case) were required, then a window would be set on a peak of interest and the accepted signals from the detector would be used to gate the brightness on an oscilloscope, whose beam was swept in synchronism with the beam of the instrument. The stored or photographed image on the screen of the oscilloscope was then a magnified image of the scanned

area - the magnification was simply the ratio of the scan amplitudes of the oscilloscope and the instrument. The principle was the same, however the scan was generated. This was the principle of the SEM and the EMP and of the Harwell PMP. It meant that data collected in spot mode were quantitative, but those collected in scanning mode were purely qualitative.

The biological work at Harwell had shown that efficiency was a major problem with the PMP. The EMP, with its much brighter beam, could achieve much better spatial resolution and still work with much higher beam currents. The PMP might be able to identify trace elements. but the requirement for thin specimens coupled with the low beam currents available meant that the counting yield for such elements was extremely low. Therefore the mapping of many individual elements required much time and subjected the specimen to very large doses of radiation. There was no evidence as to whether the elemental content and the structure were stable over such periods. Valid comparison of elemental maps also required that PMP stability be maintained over the entire period. Finally, later study of these maps and the original spectrum raised tantalising questions as to the spectra for subareas of the map corresponding to interesting features, the possibility that similar but displaced features in two maps were actually identical features in a displaced specimen, the distributions of further elements or of the same element with tighter window settings to exclude an interfering peak - questions that could be answered only by reexamination of precisely the same region of the specimen. Similar problems with the EMP had merely led to the simultaneous use of several oscilloscopes and later the use of dedicated digital stores to handle 4 maps simultaneously. This did not solve the basic problem. But what was the basic problem?

Historically, the operations of collecting a spectrum, performing a line scan and mapping had been regarded as basically unrelated activities. Given a 2-dimensional display medium, spectra were obviously quantitative; line scans could be made quantitative, by windowing the energy so that a display axis was available for the scan displacement; but maps required 2 displacement axes and hence were essentially qualitative, with the energy windowed and the intensity indicated only by point density. The problem was that these display limitations were carried over into the collection of data. When elemental maps were recorded, the scanning electronics knew the precise whereabouts of the beam spot and the detector electronics knew the precise energy of an event, but most of the energy information was thrown away. There appeared to be a conception that scanning information was essentially different from energy information, because the scan involved a physical displacement, a displacement that was continuously present, whereas the detected energy for a pulse represented a piece of data on a statistical event.

The major innovation on the Melbourne PMP was to treat the scan displacements and the energy values on an equal footing - as three pieces of coincident data per event. Then event-by-event recording of all data (as familiar in nuclear physics laboratories) could be utilised. Scanning could be continuous, since the scan position was recorded with each energy event. This enabled the introduction of fast scanning. Because computer memory was only needed to store those events which actually occurred, it was no longer necessary to set windows before collecting data - in fact it was the very essence of this system that no windows were to be set when collecting, unless to exclude an intense background of no interest. All the data on all events associated with all detectors were to be recorded.

No data were lost and, after collection, the data could be sorted into what was pictured as a 3-dimensional data block (Figure 4). Dissection of this data block then enabled all relationships between the energies and the positions of events in the 2-D scans to be established. Setting an energy window on the sorted data (A) selected an energy slice, which is an XY map of the distribution (for the element corresponding to that energy). Setting an X window and a Y window (B) selected 2 slices which intersected on a line. This produced an energy spectrum for the selected XY position. X and/or Y can be other parameters, such as angles on a goniometer. Setting an energy window and an X window (C) selected 2 slices which intersected on a line, which produced a Y spectrum. This is just an Y scan (the distribution of that element at that X value along a line in the Y direction). A line scan can be in any direction and does not have to be straight. During data collection, the total spectrum was available and maps of individual elements could be sampled with a storage oscilloscope. The system utilised a PDP11/40 computer with only 48K Bytes of memory 2 RK05 discs and a tape to handle up to 2 million events in a data block of dimensions IKxlKx8K.

Maps still included contributions from the bremsstrahlung background; but quantitative data could be extracted from any region of interest, by definition of its boundary (D). This enabled the full spectrum of events within this boundary to be extracted, a background fitted and subtracted and the areas under each peak measured. This system was described as Total Quantitative Scanning Analysis (TQSA). From its introduction (Legge, 1977; Legge and Hammond, 1979; O'Brien *et al.*, 1993), it had major effects on the efficiency of data

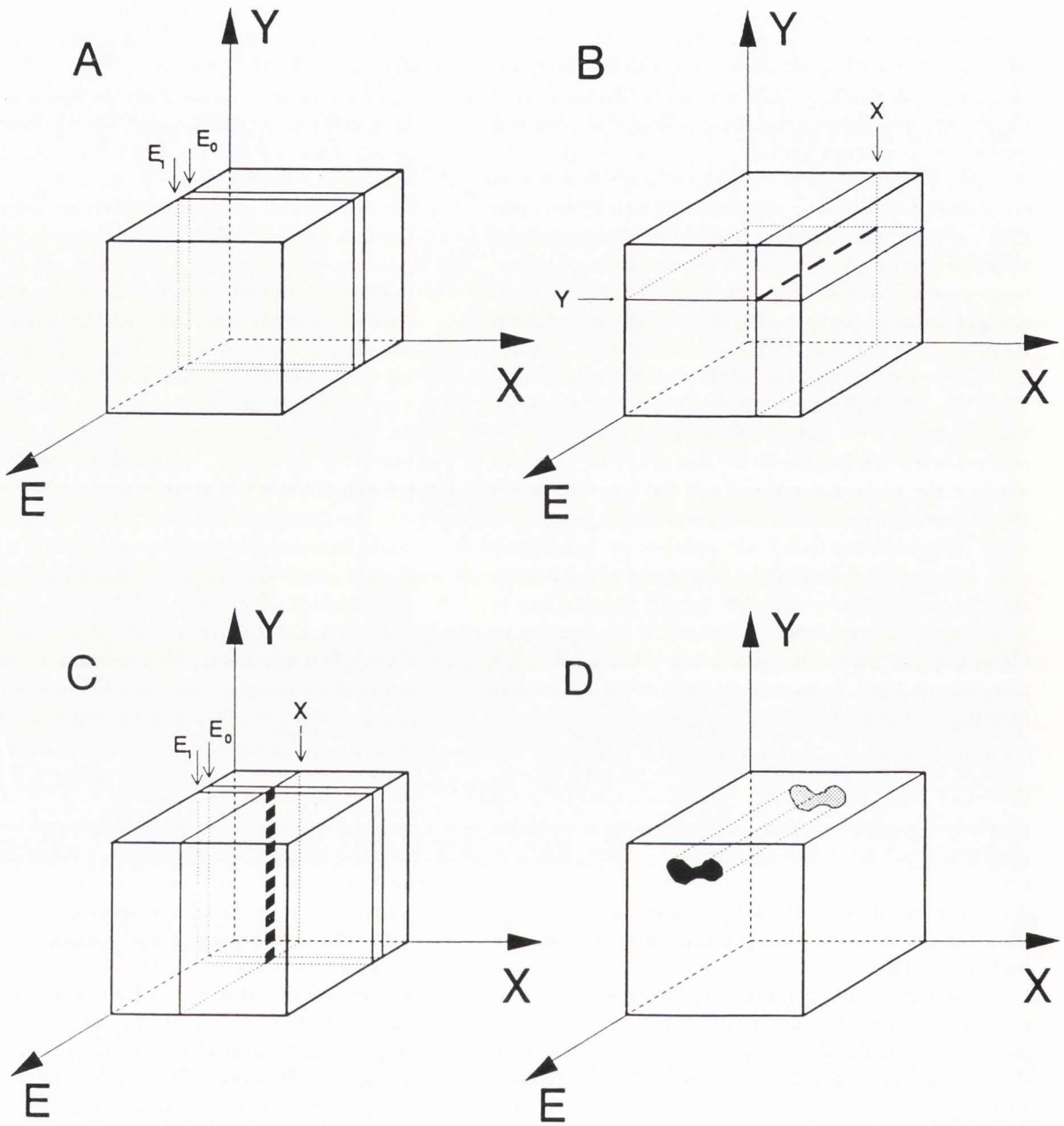

Figure 4: Representation of a 3-dimensional data block collected by TQSA technique. Dimensions are X-ray energy, beam x-displacement and beam y-displacement. The figure depicts the manner in which the block of data can be sliced or dissected to yield (A) the distribution map for any selected element, (B) the energy spectrum at any point, (C) the line scan for any element at any position and (D) the energy spectrum for any region of interest.

collection, the versatility and the quantitative power of the PMP. It also enabled the later introduction of several new techniques.

The essential features of TQSA were the permanent recording of all available data (no windowing) and the concept of the 3-dimensional data block which could be dissected and analysed at will. The use of event-by-event recording of data was the means chosen to meet the ends. because it also enabled the use of continuous scanning and the storage of data in time sequence.

Spectral recording (the direct recording of a spectrum at each pixel in turn) can be a valid approach to

TQSA. Its limitations lie in the loss of all time information and its maximisation of thermal damage. The slow scanning rate necessitated does allow the beam charge to be accurately measured for each pixel; on the other hand, this is insufficient for thin specimens, where the quantity of interest (the charge times the thickness) can only be measured by some other signal, generated from the matrix and readily available to either system. Event-by-event recording is more versatile, being able to operate in either the fast (continuous scanning) mode or the slow (stepped by charge) mode. The advantage claimed for spectral recording is efficiency in not having to store positional information. However the efficiency factor will depend on the number of events per pixel and the number of channels in the spectrum. If the spectra contain mostly channels with zero counts, then recording the number of events in each channel would be very inefficient. A compromise would be to store the energy of each event, a form of event-byevent recording in which the events are effectively presorted for x and y by collecting data in ordered sequence, though with the limitation of spectral recording to slow scanning.

The PMP was forced to adopt TQSA or some such system of efficient data handling, because of the low data rates obtained from the trace elements which it could detect. Also it could make best use of the quantitative aspects of TQSA, because of the low bremsstrahlung backgrounds in the spectra. Although TQSA was originally introduced as a method of general application to scanning instruments, it has not been adopted on the EMP until relatively recently.

Principles of Scanning

We must be careful to distinguish the way in which the scan is generated and controlled, the way in which the beam spot or stage is moved and the way in which data are recorded and handled.

In many situations it will be advantageous if the scan is under the control of a computer. It allows the beam spot to be positioned at any point of a previously scanned or aligned specimen and it allows the use of programmed scans, in which the coordinates of each scan pixel are loaded from computer memory.

We have already noted that the direct generation of all scan signals by the computer is not advisable for fast scanning, as it would tie up the computer on a routine task and also limit the possible scanning rate. The scan signals may be generated by analogue wave generators, in which case the actual coil currents or plate voltages can be sampled and digitised (by ADCs) for every event. Alternatively, digital generators may drive the computer interface directly and the deflection system through DACs.

For very large scans, it may be necessary to move the stage in order to avoid ion optical aberrations and variations in detector geometry. However one is then limited to very slow scan speeds and probably stepped scanning. Beam deflection is much faster and generally more accurate for small scans.

Free running analogue wave generators will obviously give continuous scanning; a digital scan generator can be used for continuous scanning or stepped scanning. Stepped scanning is generally advanced after the pixel has received a given beam charge, whereas continuous scanning may rely upon beam fluctuations averaging out over many passes of the beam. As discussed below, with thin specimens quantitative results in either case will require normalisation to some other signal.

A major consideration in any discussion of scanning and data collection is the question of pixel resolution and statistics. Spectral recording will normally be restricted to a small number of pixels, because of its inefficiency when the number of events per pixel is low. Event-by-event recording has no such limitation; but sometimes it is deliberately restricted in order to obtain good statistics at each pixel. In so far as it restricts the spatial resolution, this is generally not a wise move. The original TQSA concept was based on the idea that, in the normal sequence of operations, the maps of highest statistics (or some other information) are first used to define the regions of interest with resolution comparable to that of the beam spot; then complete spectra are extracted from each region of interest. Each has sufficient statistics to correct for background and normalise to some signal collected from the same region of interest. The statistics of any element in a single pixel are irrelevant. What matters is that the boundary of the region of interest can be defined as closely as possible - it may be crucial to know whether some trace element is located just outside or just inside the boundary. We are also interested in the statistics for such an element in the spectrum from the total region of interest, but those statistics are completely independent of the number of pixels used. Thus it should be beam spot resolution that decides the number of pixels to be used. If the statistics for any given map make it difficult to interpret, then it may be smoothed or summed into fewer pixels; but this should not be done during the data collection and recording process. Resolution, once sacrificed, can not be recovered.

Example of Data Handling

There are in the literature many examples of biological specimens examined in the PMP. We shall

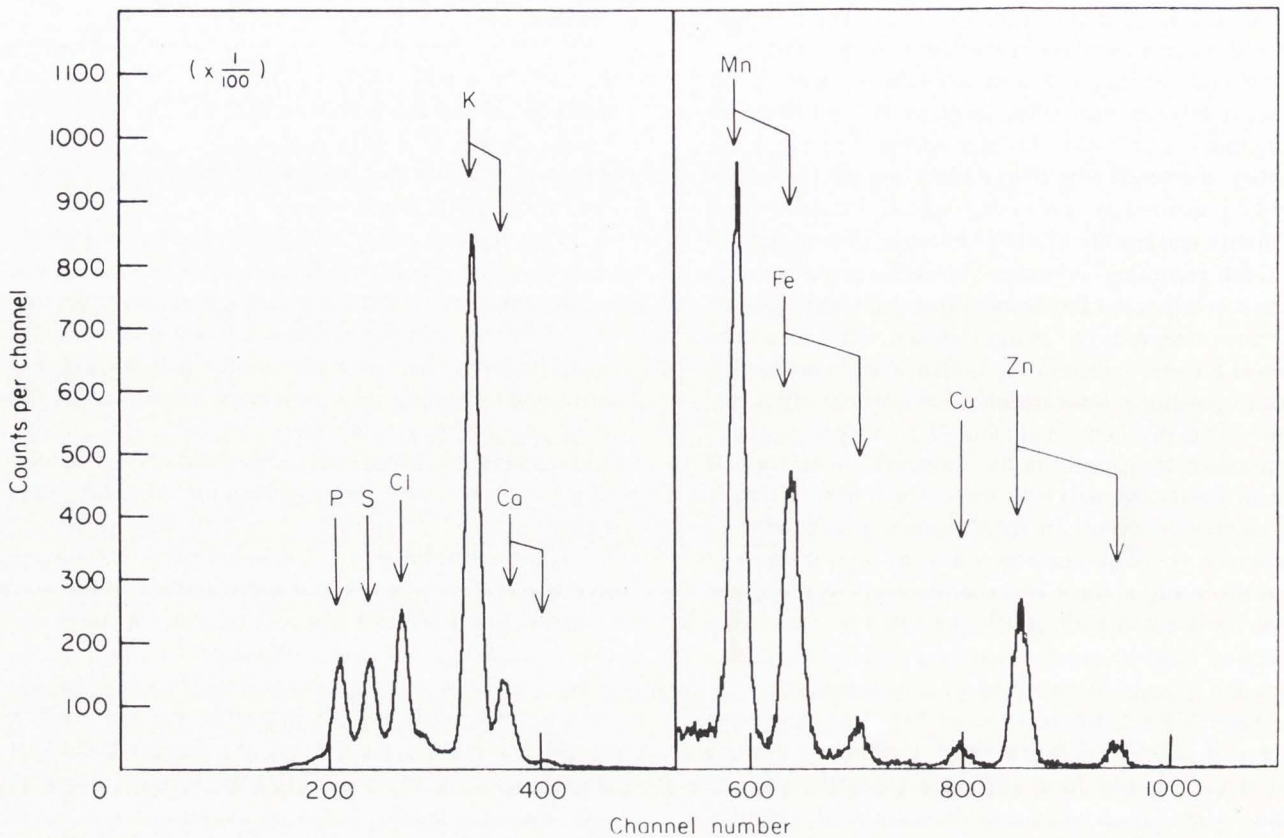

Figure 5: Spectrum of proton induced X-rays collected from the embryo region of a wheat seed. Note the change of scale for elements above Ca (Mazzolini *et al.*, 1985).

show two extreme cases - that of a relatively thick specimen and (at the conclusion of this paper) that of a very thick specimen. The same techniques are used for thin specimens.

In a study of wheat seed embryos by Mazzolini *et al.* (Mazzolini, 1985), the seeds were sectioned to 14 microns, either transversely or longitudinally, and examined in the PMP. For these measurements, the 3 MeV proton beam size was about 10 micron, the beam current 200 pA and the scan size 1.7x1.7 mm. PIXE, RBS and RFS spectra were simultaneously recorded as the specimen was scanned. The total X-ray spectrum from the sample is shown in Figure 5. This was used to select energy windows for each element of interest and these energy windows were then used to section the data block and generate the elemental distribution maps shown in Figure 6. These in turn were used to identify the regions of botanical interest. Each region was outlined, its total PIXE spectrum was extracted from the data block, its background subtracted and the yield of each element calculated. The scattered proton spectra were then used to calculate the dry weight of each region and hence normalise the measurements obtained. These are shown in Table 1. In all there were 63 quantitative measurements of elemental content per dry weight, each with its own estimated error. However they were all generated from the one scanning operation, emphasising the high information content in the data from a scanning microprobe.

These data were collected and handled with the limited computer system described above. By comparison, the memory capacity and speed available nowadays in relatively inexpensive systems are greater by two or more orders of magnitude and the system capabilities are that much greater. Data are now collected on a VME system and passed to a controlling RISC workstation for display and analysis. Recent parallel developments at many laboratories have been summarised by Lovestam (1993).

It must be remembered that any elemental maps presented on windowing the spectrum, even in a complete stored data set, will still include the contribution from any background underlying the windowed peak in the spectrum. In that sense, the maps are not quantitative, although the spectra extracted from them are. Therefore care must be taken in interpreting the map of a trace element in the spectral region of background. In rapid scanning, beam fluctuations generally average out

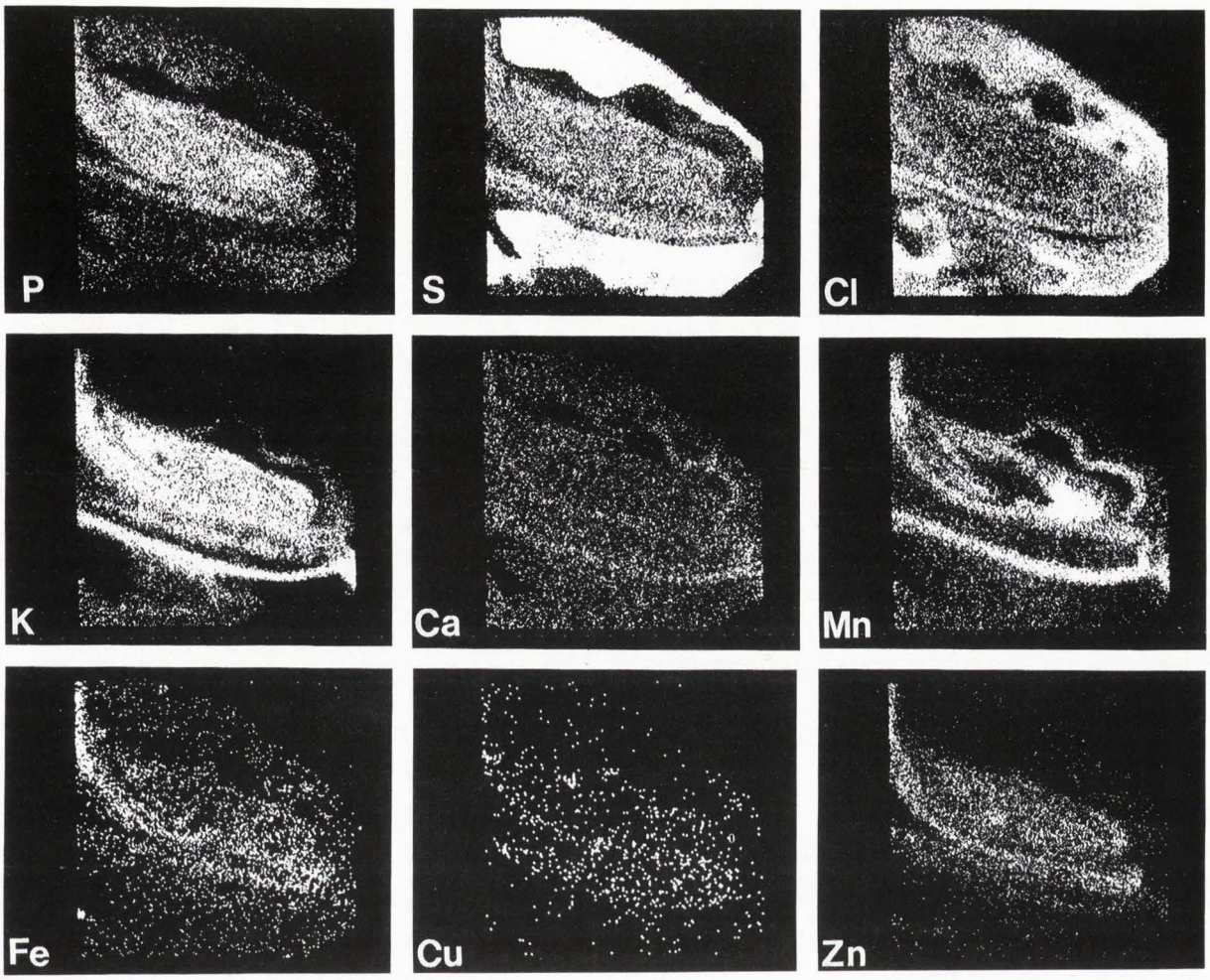

Figure 6: Distribution maps of elements in the scanned wheat seed, extracted from the data block to which the spectrum of Figure 5 belongs.

sufficiently to cause no problems with maps; but localised changes in the thickness or density of a biological specimen must be taken into account. Such changes may influence an elemental yield and any background. With all the signals available, it is possible to correct for all such influences in the spectra extracted from regions of interest. It is also possible to correct all pixels in a map by subtraction or division of a direct signal, such as that from another element and this has been done by several groups. However full correction of large high resolution maps would be very time consuming and limited by statistics. For example, with a biological sample on an organic supporting foil, full correction would require correction of an elemental signal for its background and then division by the local thickness of the sample (probably entailing a measurement of the total local thickness and a separate measurement of the foil thickness). Fortunately such work is usually not required. Recently Pallon on the Lund PMP has experimented with rapid normalisation techniques for maps where the number of pixels is limited (Pallon, 1990; Pallon and Knox, 1993).

In all the above discussion, we have not intended to rule out any system of data handling. There are many considerations in assembling a system for PMP data collection - power, resolution, quantitative accuracy, speed, efficiency, simplicity, cost, etc. We have discussed some of the principles. A major consideration not yet touched upon is versatility and this is discussed below under equipment.

Elemental Losses of Biological Specimens under Irradiation

By the time that the PMP was developed, there had been several studies of elemental losses of samples under irradiation in the EMP, notably those by Bahr (Bahr *et al.*, 1965) and by Hall (Hall and Gupta, 1974). These

Table 1. Concentrations of elements in the various regions of the embryo identified in elemental maps of Figure 6

	P	S	Cl	K	Ca	Mn	Fe	Cu	Zn
Endosperm	(8.3±5) x 10^2	(<7) x 10^2	(4.5±0.9) x 10^3	(6.2±1) x 10^3	(1±0.7) x 10^3	(3±1) x 10^1	(<4) x 10^1	(<8) x 10^0	(4±1) x 10^1
Radicle	(1.4±0.2) x 10^4	(3.8±0.7) x 10^3	(2.6±0.5) x 10^3	(2.0±0.3) x 10^4	(1.1±0.4) x 10^3	(1.4±0.2) x 10^3	(2.1±0.8) x 10^2	(2±1) x 10^1	(5.5±0.9) x 10^2
Vascular Bundle	(3±2) x 10^2	(4.4±0.7) x 10^3	(3.2±0.5) x 10^3	(1.3±0.2) x 10^4	(1.2±0.3) x 10^3	(6.0±0.9) x 10^2	(5±2) x 10^1	(4±0.8) x 10^1	(1.2±0.2) x 10^2
Scutellum	(1.4±0.2) x 10^4	(4.1±0.8) x 10^3	(2.6±0.6) x 10^3	(2.5±0.4) x 10^4	(1.1±0.6) x 10^3	(5.7±1) x 10^2	(5.7±1) x 10^2	(8±2) x 10^1	(6±1) x 10^2
Coleorhiza	(7.1±1.4) x 10^3	(4.1±0.8) x 10^3	(4.5±0.8) x 10^3	(1.7±0.3) x 10^4	(<6) x 10^2	(2±0.3) x 10^2	(1.5±0.4) x 10^2	(<4) x 10^1	(4.2±0.7) x 10^2
Leaf Primordium	(1.5±0.3) x 10^4	(3.9±0.7) x 10^3	(2.5±0.5) x 10^3	(2.1±0.4) x 10^4	(<6) x 10^2	(2.9±0.5) x 10^2	(1.5±0.4) x 10^2	(8±2) x 10^1	(4.1±0.7) x 10^2
Seed Coat	(<6) x 10^2	(9.5±2.2) x 10^2	(1±0.2) x 10^4	(6.8±1) x 10^3	(1.9±0.6) x 10^3	(5±0.9) x 10^2	(9±2) x 10^1	(1±0.5) x 10^1	(7±2) x 10^1

The data were obtained by defining each botanical region as a region of interest and extracting the associated spectrum from the data block. Normalization to dry weight was performed by simultaneously recording the light elements in the same scanned area with RBS and RFS. Errors quoted are ± SD. (All contributing errors have been added in quadrature).

authors were particularly interested in losses of the matrix material - so called mass loss. The simultaneous collection and storage of all PMP data by TQSA meant that a complete history of the irradiation was recorded. Not only could different portions of a run be inspected but, if beam charge pulses were also recorded, the yield of each element could be plotted as a function of time and any changes detected. Data collection was activated before the irradiation and effective time resolution down to about a second was obtainable (Legge, 1980; Legge and Mazzolini, 1980). This work on Mougeotia and other specimens revealed stability of most elements under normal irradiation (i.e., not an intense stationary beam spot), but a rapid loss of H in all cases, similar to that shown in Figure 7 for rat pancreatic tissue (Legge *et al.*, 1988). Since then, there have been several investigations of elemental stability under electron beam irradiation in an EMP (Egerton, 1980, 1982) and under ion beam irradiation in a PMP (Kirby and Legge, 1991; Cholewa *et al.*, 1991; Themner, 1991; Trocellier *et al.*, 1991).

The earlier biological work at Harwell was extended by Cookson, who extracted the Harwell PMP beam, to examine a cell in air (Cookson and Pilling, 1976). The collimated extracted beam of the PMP at MIT was used to examine frozen hydrated biological tissues on a cold stage (Horowitz *et al.*, 1976). This work should be mentioned because, although ionization damage is too great to allow analysis of biological tissue *in vivo* or in the normal hydrated state (and consequently biological specimens would normally have to be dried, even when working outside the vacuum), the problems are overcome with a cold stage. It is probably easier to work with such a stage outside the vacuum and there are many biological problems which require examination of frozen hydrated specimens - analysis of the elemental content of lumen, for example. On the other hand, the spatial resolution of an extracted beam will never be as good as that of the beam in vacuum. Therefore we need to develop the techniques for using cold stages in our vacuum chambers. Although several EMP groups have carried out such work and some PMP groups have proposed it, there has been no such PMP investigation to our knowledge.

Imaging

In biological work, it is essential that a microscope

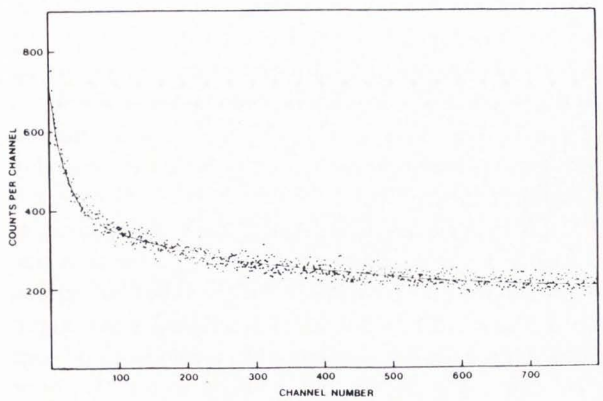

Figure 7: Rapid loss of H from a 10 micron thick, freeze dried section of rat pancreatic tissue under irradiation from a 9 nA beam of 3 MeV protons scanned rapidly over an area of 130x130 microns for 19 min (Legge *et al.*, 1988). The H losses from other organic specimens are similar.

is built into the chamber for viewing the specimen in transmission. A front viewing (reflection) microscope is also helpful, but of less Importance for biological work. Even with such equipment within the chamber, biological regions of interest may be difficult to identify and localise in the beam. Specimens should be calibrated before transfer to the microprobe chamber.

Calibration of a specimen may be done in a separate clean room - the one used for specimen preparation. The location of areas of interest on the specimen is then greatly simplified if the chamber microscope is similar to that in the clean room, both are equipped with digitally controlled stage movements, and images from each microscope can be captured with CCD cameras and by frame grabbers whose PC's are linked via ethernet to the computer or workstation used to handle PMP data, so that these images can be compared directly with each other and with other computer images, such as elemental maps.

An important step was taken by Younger and Cookson on the Harwell PMP in 1978. They utilised the ion beam to produce a secondary electron image of the specimen's surface (Younger and Cookson, 1979), much the same as was done in an EMP. Such a system has since become standard on many PMPs, giving a live image with the precise boundaries of the beam scan. It is extremely useful for location and then precise centering of the specimen or region to be studied. An image can also be stored with the other data, in order to compare with elemental maps.

Unfortunately, secondary electrons can only escape from the surface of a specimen. The resulting surface image of many biological specimens gives no indication

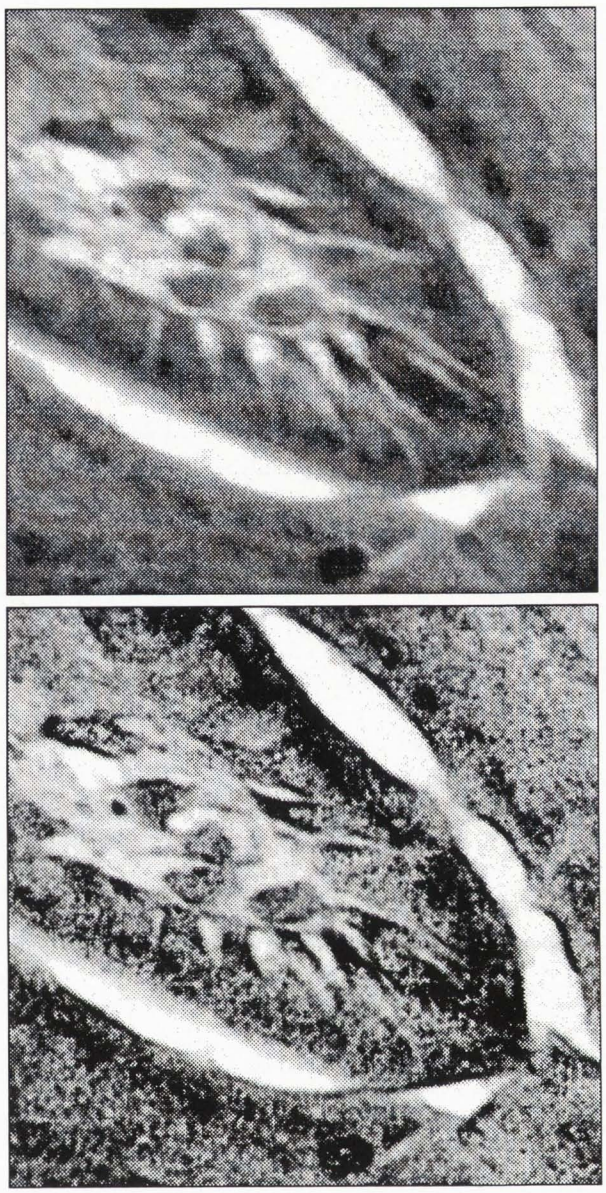

Figure 8: STIM images of a 14 micron thick section of villus tip from the ileum of a 10 day old brindled mouse. The resolution of the 2 MeV alpha particle beam was 100 nm and the scan size 68x68 micron. But these images have been compressed so that each pixel has dimensions of 250x250 nm. Image a is formed with the median of all energies recorded at each pixel. Image b is formed from the lower second moment at each pixel of the same data set (Bench *et al.*, 1991).

of internal structure. Even the light optical transmission image of an unstained freezedried specimen is often featureless. In the case of sections taken on a cryomicrotome, it is possible to stain the sections on either side of the section examined in the beam, a technique well known in electron microscopy. However it is a specia-

lised technique and does not help in positioning a sample for irradiation. It also relies upon the same structure appearing in adjacent sections. This does not always occur with fine structure in the thick (several micron) sections utilised in a PMP. A second problem with imaging is the need for high resolution. Sometimes a high resolution image of fine structure is needed in order to identify the nature of much larger structure that is to be analysed. The PMP did not have a high contrast imaging tool comparable to STEM, which Hall was then using to good effect on the EMP.

It was these two problems that led to the search for a new, independent imaging technique that would give good contrast at high resolution very quickly. The solution, as with STEM, was to use the primary ion beam, rather than secondary radiation such as X-rays or electrons. In this technique, known as scanning transmission ion microscopy (STIM), Sealock *et al.* reduced the beam current to about 1000 ions per second, by reduction of the object and aperture diaphragms, thus reducing the first order beam spot size and the aberrations. A detector placed at 0° measured the energy loss of the transmitted ions and the TQSA system was used to collect a data block as usual. This was windowed to show slices of different specimen thickness or areal density at resolutions better than 500 nm (Sealock *et al.*, 1983, 1987). Contrast is given by the energy loss or by scattering out of the direct beam and may be observed by measuring the direct beam (bright field), as above, or by using an annular collimator to measure the beam scattered at small angles (dark field).

Coincident with the above work, Overley *et al.* used the IMP at Eugene in a similar manner to make radiographs of biological structure. The resolution was only 5 micron but their initial investigation and publication was much more thorough (Overley *et al.*, 1983). It was simple at Melbourne to utilise the TQSA system to display slices of the data block, corresponding to various thickness contours of the specimen. Overley *et al.* had no such system and, since there can be only one true thickness at any point, they represented all thicknesses of the sample on the one map by displaying the measured energy loss at each point with a grey scale image (Lefevre *et al.*, 1987). This produced a good contrast image. Furthermore, Overley *et al.* showed that the contrast could be improved by averaging several measurements at each point and that the median was a better parameter than the mean, because it gave less weight to spurious events. Finally, at Eugene the scan was stepped, with advancement to the next pixel after an event was recorded, whereas at Melbourne the continuous scanning system produced a random number of events per pixel. With TQSA it is still possible to form and display the median, and this is now done at Melbourne on line, as data are collected, a stepped scan now being adopted for such STIM measurements. Figure 8a shows the contrast that can be obtained and the detail that can be seen in a STIM image. It is a 14 micron thick, freeze dried cryosection of villus tip from 10 day old brindled mouse ileum, from a study by Kirby *et al.* (1991). The beam was 0.2 fA of 2 MeV alpha particles focussed to a spot of diameter 100 nm and the scan size was 68x68 micron. We can see the brush border, lamina propria, basal membrane, goblet cell and some dense subcellular localisations. None of this detail can be seen in an elemental X-ray image, because of the poor statistics and inferior spatial resolution.

STIM has provided the fast, high resolution, high contrast imaging technique that was needed with biological specimens and several PMP laboratories have adopted it. It does require a separate measurement, but arrangements can be made to perform this rapidly. It is not going to answer all imaging problems and there is need for more work in this regard. STIM itself has more to offer than a direct energy loss or scattering contrast image.

There was yet another major point made in the above paper by Overley *et al.*- they remarked that the distribution of events about the mean might indicate whether unresolved spatial structure existed in the sample. This gave another example of the strength of TQSA, for which all data events can be recorded. The TQSA system at Melbourne was utilised to test the proposal from Eugene on some old recorded Melbourne data, with dramatic results. Figure 8b shows the result when the same data set as seen in Figure 8a is used to map the lower second moment (Bench *et al.*, 1991). We now see the brush border standing out strongly, and structure is observed within the goblet and other cells. This technique shows the presence of density variations associated with pores, granules or fine structure smaller than the beam resolution.

With STIM, the initial emphasis at Melbourne was on high spatial resolution of imaging and this has been reduced to 50 nm (Bench and Legge, 1989). At Eugene the emphasis was on quantitative mass measurement, and its use to normalise PIXE measurements, pixel by pixel. It is a useful technique for quantisation; but it must be remembered to reduce the STIM map to the same spatial resolution as the PIXE map (by smoothing if necessary), or spurious structure will result. STIM imaging, including stereo imaging, has been reviewed by Lefevre *et al.* (Lefevre *et al.*, 1991).

At this point mention must be made of much earlier work by Armitage *et al.* at Harwell (1975). Using a collimated beam, they measured energy straggling in

both transmission and resonant backscattering of ions and showed that they could thus determine the porosity of materials. Also STIM had been employed as early as 1978 by Levi-Setti and Fox with low energy (keV) ions (Levi-Setti and Fox, 1980). There is now a rapidly growing literature on STIM and related techniques.

TQSA enabled the development of channelling contrast microscopy (CCM) in 1982 (McCallum *et al.*, 1983) and channelling STIM in 1989 (Cholewa *et al.*, 1990). Both are powerful techniques for materials analysis and have been extended to geological analysis (Jamieson and Ryan, 1993). We may later see them applied to the analysis of organic crystals. The ability to control single ions was first developed by Fischer at Darmstadt, using similar ion optical techniques, with added instrumentation for the control and detection of the ions (Fischer, 1988, 1991). This has opened up a wide range of studies with single event upsets in the field of semiconductors and, more importantly to this review, the possibility of directing controlled numbers of ions to specific points in a cell *in vivo* and studying the resultant genetic evolution (Geard *et al.*, 1991).

Tomography

The Annual Report on 1983 Work at G.S.I. Darmstadt described work on STIM with heavy ion beams by Fischer, who followed it with two-dimensional STIM tomography in 1988 (Fischer and Muhlbauer, 1990). STIM tomography with protons had been reported at high energies (25 MeV) and low spatial resolution (100 micron) by Ito and Koyama-Ito in 1984 (Ito and Koyama-Ito, 1984). 1988 also saw the first three-dimensional STIM tomography carried out at the Lawrence Livermore Laboratory by a team from Sandia and Lawrence Livermore Laboratories (Pontau *et al.*, 1989). Pontau and others of the Sandia group have collected three-dimensional STIM tomographic information and utilised powerful software developed at Livermore for handling three dimensional tomographic images. They have collaborated with the Melbourne PMP group to produce three-dimensional tomographs at high resolution (Bench *et al.*, 1992). This is proving to be a very powerful analytic tool in its own right, having about an order of magnitude higher spatial resolution than the corresponding X-ray tomographs from synchrotron radiation. Computer images have been constructed with three-dimensional spatial resolution of 250 nm and, for small specimens, finer resolution should be possible.

We shall give one example of the microprobe used as a microscope to examine three-dimensional structure in a relatively large specimen (Bench *et al.*, 1992). The specimen is a pollen grain of *Lilium longiflorum*. This botanical species has been examined in cross section several times in PMPs by Reiss, first with Nobiling and Traxel at Heidelberg (Ender *et al.*, 1983), then with Watt and Grime at Oxford (Reiss *et al.*, 1985) and finally with Traxel again at Heidelberg (Reiss and Traxel). In those studies, the interest was in the elemental movements and concentrations during germination. In this study, we are looking at the 3-D structure of the grain before germination. A fresh pollen grain was dehydrated for three days at 20°C, critical point dried and mounted on the tip of a micropipette attached to a 360° goniometer.

A beam of 3 MeV protons focused to a spot of 400 nm diameter was scanned over an area of 96x84 micron containing the 80 micron grain and the bright-field, energy-loss STIM image was recorded in 256x256 resels. (A resel, or resolution element, is commonly used in tomography to denote an element in the collected raw data, as distinct from an element in the computed image data, which is termed a pixel, or picture element.) The energy loss recorded for each resel was the median value from 7 measurements (that is the passage of seven ions). Figure 9 shows a stereo pair of such images. From the outline of the grain, we can clearly see that there is structure on its surface (the so-called sculpturing, characteristic of each type of grain) and within the grain there is some dense structure which cannot be clearly resolved.

The above procedure was repeated for 400 angles evenly spaced over a 180° rotation of the goniometer. Each projection was corrected for any irregularities in the movement of the goniometer. The data were converted from energy loss to density, by assuming an average composition of $Cl_{12}NO_4H_{24}$. This composition was determined by recording the RBS spectrum from the grain, which gave a measurement of the C, N and O contents. From an assumption that the major constituents would be starch, cellulose, lipids and water, the hydrogen content could then be estimated with sufficient accuracy by the method of Mazzolini *et al.* (Mazzolini, 1985).

Filtered back projection was then used to construct a tomogram of 256 slices, which revealed sharp structure which repeats in adjacent slices. Figure 10a is a composite of all slices, with the transparency adjusted to emphasise surface features. In Figure 10b, the same view is presented, but with transparency adjusted to reveal some of the internal structures, notably the two nuclei (vegetative and generative) which are an essential feature of such pollen grains. These structures can be adequately studied only in the 3-D image which, when formed can then be rotated and visually dissected. Figure 10c shows the same data rotated and viewed from

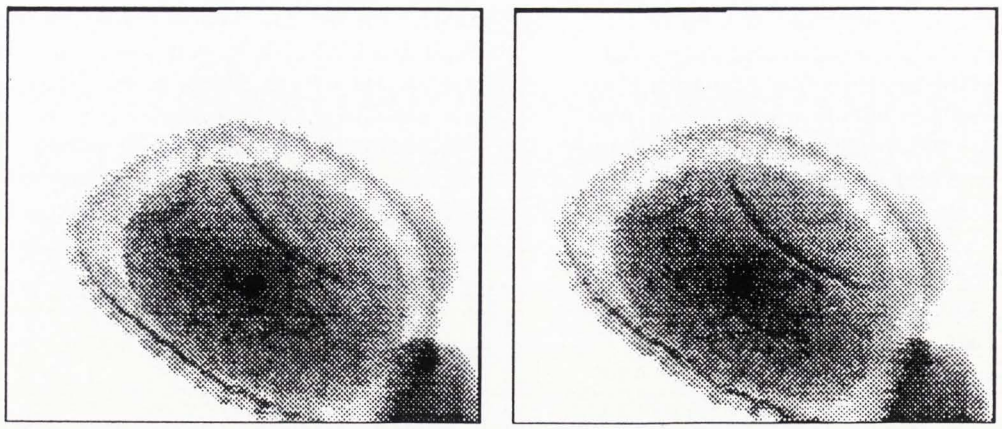

Figure 9: STIM energy loss images (projections) of an unsectioned pollen grain of *Lilium longiflorum* (Bench *et al.*, 1992). The 96x84 micron scan is distributed over 256x256 resels. Surface sculpturing is visible but the internal structure (nuclei) can not be clearly resolved in this 80 micron thick specimen. The two images are projections at 4° spacing, forming a stereo pair.

a different direction. The top of the data block has been removed as it included the glue attaching the pollen grain to the micropipette (visible at the top Figure 9).

Three-dimensional STIM tomography is extremely demanding of computer speed and storage. For example, the analysis of a sample of only 50 micron dimensions, to an accuracy of 50 nm, would require that a scan of 1Kx1K pixels be repeated for about 2K individual projection angles. In order to achieve a thickness sensitivity of about 50 nm, the median of about 10 measurements per pixel must be taken. Thus we would require about $2x10^{10}$ events. At 10 K events per second we would need a total experimental run time of 2M seconds or about 600 hours. If the data were preprocessed and only the median values stored, we would have to store 4 GB of data. The 4 GB data block would then have to be processed in 4 MB arrays, before combining these in slices, in order to produce the final 3-D image of 2 GB. Run times can be decreased by increasing the data collection rate; but that increases the demands on preprocessing speed and does not relieve the demands on data storage and array handling.

Whereas it is valuable to be able to examine the physical structure of intact 3-dimensional objects, of possibly even greater value would be an ability to examine their elemental nature in 3 dimensions. Two preliminary investigations with PIXE Tomography (PIXET) have been made. Schofield and Lefevre have formed a 2-dimensional tomograph incorporating some of the corrections needed (Schofield and Lefevre, 1993). Saint *et al.* have examined a 3-dimensional data set and discussed the necessary corrections (Saint *et al.*, 1993). These corrections are challenging - the ion beam loses energy as it penetrates the specimen and hence the cross section for X-ray production is a function of depth and the ion's path; the X-rays are absorbed as they pass through the specimen and hence the efficiency of collection depends on the point of origin of the X-ray and its chosen path through the specimen to the detector. Thus integration over the volume of the specimen and the area of the detector is required. It is proposed that a STIM tomograph be combined with the PIXET measurement, if necessary in an iterative manner, in order to extract accurate 3-D tomographs for each element. In tomography, the high penetrability of energetic ions, previously seen as a disadvantage because of superposition of structure in thick specimens, becomes a useful property. The ion and its energy may be selected to suit the specimen thickness and density.

Equipment

The control of a PMP may be conveniently integrated into the data handling system, by handling both with the one VME computer system, running under some multitasking operating system, or by the use of several PCs linked by ethernet. Overall control can be exerted from a central computer or workstation, from which the beam or the specimen may be moved or a scan of either may be initiated. Fast scanning of the beam is possible if the digital scan generator is an independent module, though under computer control. Digital lens control likewise can be an independently running process, though under the overall control of the operator. Such a system makes incorporation of further experimental operations relatively straightforward.

Much more so than the EMP, the PMP may be said to be a computer based instrument. The computer is at

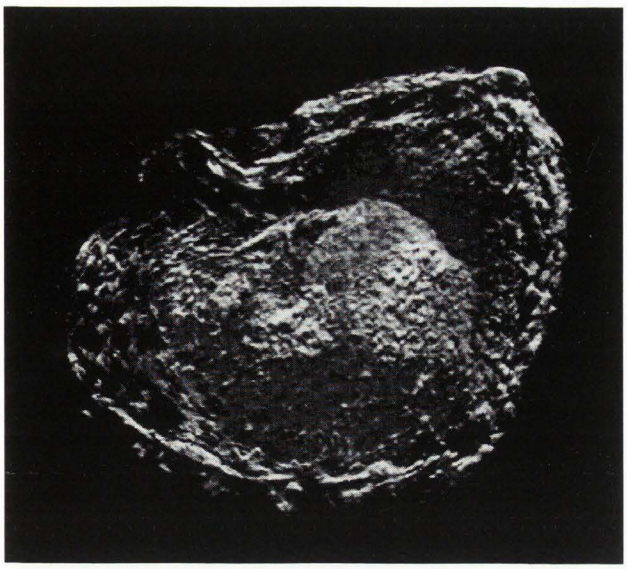

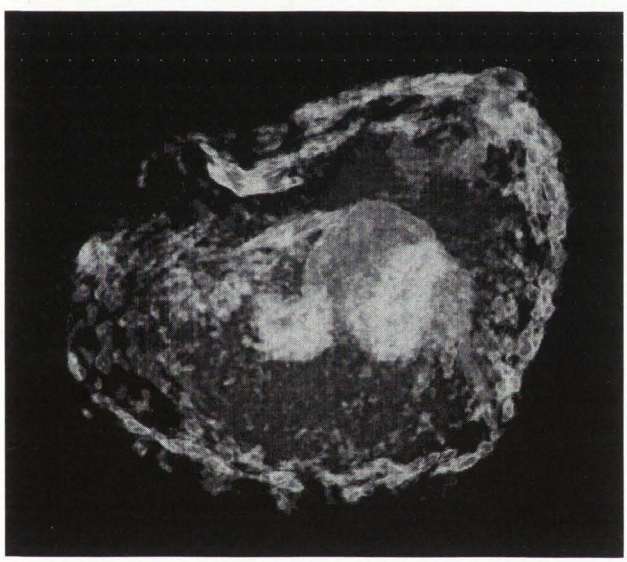

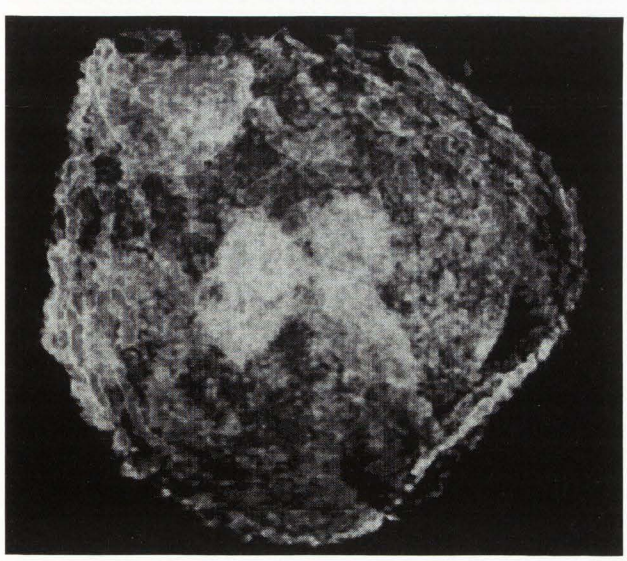

Figure 10: 3-dimensional tomograph of 256 slices, formed from a complete set of 400 projections, taken at 400 angles over 180°, two of which are shown in Figure 9. a and b show a composite view of all slices, with the transparency adjusted to emphasise surface features (a) or internal structure (b). c shows the same tomograph viewed from a different direction.

the heart of data collection as well as all subsequent data handling procedures. In many cases, it will determine the measurements that can be made, as well as the data rates achievable. Sometimes it has been claimed that data must be windowed, or restricted in other ways, to proportions manageable by the computer. An example has been given of the possible demands in three-dimensional STIM tomography. However it must be pointed out that the computer hardware available at any given time has always been able to meet the demands of PMP data recording, as these demands have rapidly escalated. We are very wary of any form of enforced windowing of the incoming data. Rapid recording, sorting and display of multidimensional data is possible. We believe, with microprobes in general, the limitations will always be in the microprobe beam, the detectors and their electronic systems - not the data handling systems.

Acknowledgements

In this paper, we have attempted to show how biological work with the PMP was built on that which preceded it with the EMP. Much of the pioneering work in the latter field had been done by the Cambridge EMP group with T.A. Hall and he provided valuable guidance for the development of appropriate techniques on the PMP for which we shall always be grateful.

We also acknowledge the work of many who contributed to the work of our own group (especially G. Bench) and would emphasise that, in illustrating and discussing techniques and their development, we have not attempted to cover the wide spectrum of biological applications seen in the contributions from many laboratories.

We particularly thank Phil Taylor of the Department of Botany, University of Melbourne, who prepared the pollen grain sample and assisted in the interpretation of data and Drs Hammond and Whitehouse of the Research School of Physical Sciences, ANU, who analysed the tomographic data - work to be published elsewhere.

We acknowledge the support of the Australian Research Council.

References

Allan GL, Camakaris J, Legge GJF (1991) The elemental analysis of normal and Menkes fibroblast cells with the SPMP. Nucl Instr Meth **B54**: 175-179.

Armitage BH, Trehan PN, Porter DR, McKenzie CD (1975) Pore size measurement using charged particle beams. Harwell Report AERE-PR/NP22: 60-63.

Bahr GF, Johnson FB, Zeitler E (1965) Lab Invest **14**: 1115.

Bench G, Legge GJF (1989) High resolution STIM. Nucl Instr Meth **B40/41**: 655-658.

Bench G, Lefevre HW, Legge GJF (1991) The mapping of unresolved spatial structure in STIM images. Nucl Instr Meth **B54**: 378-382.

Bench G, Saint A, Cholewa M, Legge GJF, Weirup DL, Pontau AE (1992) STIM tomography: a three-dimensional high resolution imaging tool. Nucl Instr Meth **B68**: 481-490.

Brune D, Lindh U, Lorenzen J (1977) A proton semi-microbeam device for surface analysis. Nucl Instr Meth **142**: 51-54.

Cho ZH, Singh M, Mohabbatizadeh A (1974) Biomedical applications and instrumental implications of ion microprobe. IEEE Trans Nucl Sci **NS-21**: 622-627.

Cholewa M, Bench G, Kirby BJ, Legge GJF (1991) Changes in organic materials with scanning particle microbeams. Nucl Instr Meth **B54**: 101-108.

Cholewa M, Bench G, Legge GJF, Saint A (1990) Channeling scanning transmission ion microscopy. Appl Phys Lett **56**: 1236-1238.

Cookson JA, Pilling FD (1970) A 3 MeV proton beam of less than four microns diameter. Harwell Rept AERE - R 6300.

Cookson JA, Ferguson ATG, Pilling FD (1972) Proton microbeams, their production and use. J Radioanalyt Techniques **12**: 39-52.

Cookson JA, Pilling FD (1976) Proton microbeam analysis in air. Phys Med Biol **21**: 965-969.

Cookson JR, Legge GJF (1975) Biological analysis with a nuclear microprobe. Proc Analyt Div Chem Soc **August**: 225-229.

Coote GE, Sparks RJ (1981) Fluorine concentration profiles in archeological bone: an application of a nuclear microprobe. NZJ Archeology **3**: 21-32.

Coote GE, Sparks RJ, Pohl KP, West JG, Purcell CR (1978) Inst Nuc Sci D.S.I.R. Rpt. INS-R-242, 10.

Dymnikov AD, Yavor SYA (1963) Four quadruple lenses as an analog of an axially symmetric system. Zhurnal Tekhnicheskoi Fiziki **33**: 851-858.

Echlin P, Moreton R (1974) The preparation of biological materials for x-ray microanalysis. In: *Microprobe analysis as applied to cells and tissues* (Hall T, Echlin P, Kaufmann R, eds), Academic Press, London and New York, pp 159-174.

Egerton RF (1980) Measurement of radiation damage by electron energy-loss spectroscopy. J Microsc **118**: 389.

Egerton RF (1982) Organic mass loss at 100 K and 300 K. J Microsc **126**: 95-100.

Ender Ch, Li MQ, Martin B, Nobiling R, Povh B, Reiss H-D, Traxel K (1983) Demonstration of polar zinc distribution in pollen tubes of *Lilium longiflorum* with the Heidelberg proton microprobe. Protoplasma **116**: 201-203.

Fischer B (1988) The heavy ion microprobe at GSI - used for single ion micromechanics. Nucl Instr Meth **B30**: 284-288.

Fischer B (1991) Single particle techniques. Nucl Instr Meth **B54**: 401-406.

Fischer B, Muhlbauer C (1990) Microtomography by heavy ions. Nucl Instr Meth **B47**:271 -282.

Folkmann F, Gaarde C, Huus T, Kemp K (1974a) Proton induced X-ray emission as a tool for trace element analysis. Nucl Instr Meth **116**: 487-499.

Folkmann F, Borggreen J, Kjeldgaard A (1974b) Sensitivity in trace elemental analysis by p,a and 160 induced X-rays. Nucl Instr Meth **119**: 117-123.

Geard CR, Brenner DJ, Randers-Pehrson G, Marino SA (1991) Single particle irradiation of mammalian cells at the Radiological Accelerator Research Facility: induction of chromosomal changes. Nucl Instr Meth **B54**: 411-416.

Guy J (1977) Continuous x-ray spectrum from proton interactions with matter. 4th Year Report, School of Physics, University of Melbourne (unpublished).

Hall TA (1968) Some aspects of the microprobe analysis of biological specimens. In: *Quantitative Electron Microprobe Analysis* (Heinrich FJ, ed), NBS Special Publ **298**: 269-299.

Hall TA, Gupta BL (1974) Beam-induced loss of organic mass under electron microprobe conditions. J Microsc **100**: 177-188.

Heck D (1979) The Karlsruhe proton microbeam system. Beitr Elektronenmikroskop Direktabb Oberfl **12/1**: 259-262.

Horowitz P, Aronson M, Grodzins L, Ladd W, Ryan J, Merriam J, Lechene C (1976) Elemental analysis of biological specimens in air with a proton microprobe. Science **194**: 1162-1165.

Ito A, Koyama-Ito H (1984) Possible use of proton CT as a means of density normalization in the PIXE semi-microprobe analysis. Nucl Instr Meth **B3**: 584-588.

Jamieson DN, Ryan CG (1993) Microprobe channelling analysis of pyrite crystals. Nucl Instr Meth **B77**: 415-421.

Kirby BJ, Legge GJF (1991) Ion beam induced damage and element loss during a microanalysis of biological tissue. Nucl Instr Meth **B54**: 98-100.

Kirby BJ, Legge GJF (1993) The preparation of biological tissue for a trace element analysis on the proton microprobe. Nucl Instr Meth **B77**: 268-274.

Kirby BJ, McArdle H, Danks DM, Legge GJF (1991) Distribution of trace elements in normal and diseased mouse ileum and kidney tissues. Nucl Instr Meth **B54**: 171-174.

Lefevre HW, Schofield RMS, Overley JC, McDonald JD (1987) Scanning transmission ion microscopy. Scanning Microsc **1**: 879-889.

Lefevre HW, Schofield RMS, Bench GS, Legge GJF (1991) STIM with energy loss contrast: an imaging modality unique to MeV ions. Nucl Instr Meth **B54**: 363-370.

Legge GJF (1974) Biological studies. Harwell Rept. AERE - PR/NP 21, 66 and Elemental microanalysis of cells using a proton microbeam. Proc Roy Micr Soc **9**: 45.

Legge GJF (1977) Some experiments with a proton microbeam. Abstr 48th ANZAAS Congress, p. 25.

Legge GJF (1980) The scanning proton microprobe. In: *Microbeam Analysis 1980* (Wittry DB, ed), San Francisco Press, San Francisco, pp 70-76.

Legge GJF, Hammond I (1979) Total quantitative recording of elemental maps and spectra with a scanning microprobe. J Microsc **117**: 201-210.

Legge GJF, Mazzolini AP (1980) Elemental microanalysis of biological and medical specimens with a scanning proton microprobe. Nucl Instr Meth **168**: 563-569.

Legge GJF, McKenzie CD, Mazzolini AP (1979) The Melbourne proton microprobe. J Microsc **117**: 185-200.

Legge GJF, Mazzolini AP, Roczniok AF, O'Brien PM (1982) Application of a scanning proton microprobe to biology and medicine. Nucl Instr Meth **197**: 191-200.

Legge GJF, O'Brien PM, Kirby BJ, Allan GL (1988) Proton microscopy and microanalysis. Ultramicroscopy **24**: 283-298.

Levi-Setti R, Fox TR (1980) High resolution scanning ion probes: applications to physics and biology. Nucl Instr Meth **168**: 139-149.

Lindh U (1988) Medical applications of the nuclear microprobe. Nucl Instr Meth **B30**: 404-416.

Lindh U (1991) Nuclear microscopy. Its role and future in medicine and trace element biology. Nucl Instr Meth **B54**: 160-170.

Lindh U, Brune D, Nordberg D (1978) Microprobe analysis of lead in human femurby proton induced x-ray emission (PIXE). Sci Total Environm **10**: 31.

Lovestam NEG (1993) Currently used control and data acquisition systems for nuclear microprobes. Nucl Instr Meth **B77**: 78-83.

Mak BK, Bird JR, Sabine TM (1966) Proton microanalysis. Nature **211**: 738-739.

Malmqvist KG (1986) Proton microprobe analysis in biology. Scanning Microsc **3**: 821-845.

Mazzolini AP, Pallaghy CK, Legge GJF (1985) Quantitative microanalysis of Mn, Zn and other elements in mature wheat seed. New Phytol **100**: 483-509.

McCallum JC, McKenzie CD, Lucas MA, Rossiter KG, Short KT, Williams, JS (1983) Channeling contrast microscopy: application to semiconductor structures. Appl Phys Lett **42**: 827-829.

Nobiling R, Traxel K, Bosch F, Civelekoglu Y, Martin B, Povh B, Schwalm D (1977) Focussing of proton beams to micrometer dimensions. Nucl Instr Meth **142**: 49-50.

O'Brien PM, Moloney G, O'Connor A, Legge GJF (1993) A versatile system for the rapid collection, handling and graphics analysis of multidimensional data. Nucl Instr Meth **B77**: 52-55.

Overley JC, Connoly RC, Sieger GE, McDonald JD, Lefevre HW (1983) Energy-loss radiography with a scanning MeV-ion microprobe. Nucl Instr Meth **218**: 43-46.

Pallon J (1990) A scanning proton microprobe data sorting and display system. Nucl Instr Meth **B44**: 377-391.

Pallon J, Knox (1993) Quantitative elemental mapping of biomedical specimens using the nuclear microprobe. Scanning Microsc **7**: 1207-1214.

Pierce TB, Peck PF, Cuff DRA (1966) Examination of surfaces by scanning with charged particles. Nature **211**: 66-67.

Pierce TB, Peck PF, Cuff DRA (1968) The microanalysis of surfaces by scanning with charged particle beams. Nucl Instr Meth **67**: 1-8.

Pontau AE, Antolak AJ, Morse DH, Ver Berkmoes AA, Brase JM, Heikkinen DW, Martz HE, Proctor ID (1989) Ion microbeam tomography. Nucl Instr Meth **B40/41**: 646-650.

Price PB, Bird JR (1969) Proton microanalysis. Nucl Instr Meth **69**: 277-281.

Wilde HR, Roth M, Uhlhorn CD, Gonsior B (1978) Analysis of the lateral distribution of trace elements in biological and other materials by proton-induced x-ray fluorescence using a microbeam scanner. Nucl Instr Meth **149**: 675-678.

Reiss H-D, Grime GW, Li MQ, Watt F, Takacs J (1985) Protoplasma **126**: 147.

Saint A, Cholewa M, Legge GJF (1993) PIXE Tomography. Nucl Instr Meth **B75**: 504-510.

Schofield MS, Lefevre HW (1993) STIM-PIXE microtomography. Nucl Instr Meth **B77**: 217-224.

Sealock RM, Jamieson DN, Legge GJF (1987) Scanning transmission microscopy with a 2 MeV alpha particle microbeam. Nucl Instr Meth **B29**: 557-566.

Sealock RM, Mazzolini AP, Legge GJF (1983) The use of He microbeams for light element x-ray analysis of biological tissue. Nucl Instr Meth **218**: 217-220.

Themner K (1991) Elemental losses from organic material caused by proton irradiation. Nucl Instr Meth **B54**: 115-117.

Trocellier P, Tirara J, Massiot P, Gosset J, Constantini JM (1991) Nuclear microprobe study of the composition degradation induced in polyimides by irradiation with high-energy heavy ions. Nucl Instr Meth **B54**: 118-122.

Watt F, Grime GW (1988) Elemental mapping of biological samples using a scanning proton microprobe. Nucl Instr Meth **B30**: 356-366.

Younger PA, Cookson JA (1979) A secondary electron imaging system for a nuclear microprobe. Nucl Instr Meth **158**: 193-198.

Discussion with Reviewers

J. Pallon: Many of the subjects you discuss in this paper are now well established techniques and used as standard methods in the modern microprobe laboratory. The exception is the technique for tomography, and especially PIXE tomography, which mainly has been used in a demonstrative manner. If there will be a breakthrough for tomography, in what fields of biology/medicine do you expect the most likely applications to fall? Expressed in another way, in what type of fields would you prefer to irradiate a sample 1 - 3 weeks instead of cutting it into small sections and spend 3 hours of beam time on each section?

Authors: Your comment is true; but techniques follow a common path of acceptance and it is relevant to note that when CCM, STIM and CSTIM were introduced, each technique, in turn, met with the comment that it was an interesting demonstration, but would it ever be useful - this despite the fact that each had been introduced in order to meet a specific need. It is not a breakthrough that brings general acceptance and wide usage, but simply the gradual tooling up of laboratories to handle and exploit a new technique. Tomography will probably follow the same path. It has already been demonstrated that, for many specimens, STIM tomography is able to provide better resolution and greater density contrast than X-ray microtomography or any other technique. Its place in the physical sciences is established. In the biological sciences, it again fills the gap between electron microtomography for thin specimens and hard X-ray microtomography for thick ones. The alternative technique of serial sectioning is often problematic. Fixation is a problem for all techniques, because of the need to preserve morphology without change of density (the parameter measured by STIM). Sectioning brings the added danger of deformation, which may be severe, unless embedding is used with consequent problems in the measurement of density.

STIM tomography is needed in determining how the properties of materials depend on density distributions within the organic fibres of their constituents. It may be needed in the morphological study of complex opaque structures; but, generally, its principle strength is the accurate determination of 3-D density distributions.

The next decade will see improvements in the techniques of collecting and handling large data files, to give much greater efficiency and pixel resolution, without the need to irradiate for days. This will be particularly important to PIXE tomography, which, we agree, is still in the demonstration stage and the early development stage. Limited angle tomography will also benefit from intensive investigation, opening the way for PIXE analysis of biological sections with good depth resolution. There are many artifacts in tomography and PIXE tomography has the added problem of multiple corrections, which must be applied iteratively. However, serial sectioning is even more problematic for PIXE work, because the simultaneous preservation of precise morphology and of elemental content is extremely difficult. In summary, tomography is a very general technique and its applications will lie in all fields where precise multiple serial sectioning with preservation of relevant information is difficult.

J. Pallon: When comparing the use of the electron and proton microprobe, it is obvious that the EMP serves as a routine instrument while the PMP is still a research facility. What type of modifications or developments of the PMP must take place in order to make it more attractive for use within medicine/biology? Are the changes to be found in the instrumentation, or is it a matter of lacking communication?

Authors: This is an important but complex question.

With the development of the Si(Li) detector for X-rays, the EMP became a routine instrument in medicine/biology, because it was able to tackle routine problems and solve them rapidly and because it could be realized by simply adding a Si(Li) detector to a commonly used instrument, the SEM. For trace element analysis, the wavelength dispersive detector (crystal spectrometer) was still required and this has remained more of a research instrument. In contrast to the EMP,

the PMP is not needed for routine (non-trace) elemental microanalysis in medicine/biology and, being more expensive and complex, is not likely to become a routine instrument in this field. However, its sensitivity to trace elements, quantitative accuracy, instrumental development and versatility with multiple techniques (many of which can be combined) should lead to its much wider use within the research area. There are three factors which often inhibit this development:

(i) The low brightness of present accelerator beams leads to lengthy analysis times for trace elements. In contrast, the EMP, which routinely looks only for major and minor elements, has a much brighter beam and its users have learned to cope with the associated specimen damage.

(ii) The PMP and its associated accelerator could be simplified in their operation, but some of the complexity could be removed only with the sacrifice of versatility. It must be remembered also that most biological scientists do not have (and do not wish to have) the familiarity with complex instrumentation possessed by many physical scientists. Close collaboration is needed between physicists and biologists.

(iii) The PMP must be seen, not as an expensive alternative to the EMP for routine elemental microanalysis, but as an indispensable tool for trace elemental microanalysis and some other microanalytical problems. In order to gain acceptance for the PMP in medicine/biology, it is most important to demonstrate and emphasise its applicability in appropriate key areas, as has been done by some groups. This paper has made no attempt to cover such developments but reference should be made to other papers in the proceedings of this conference.